Calibration and Validation of ASCAT Winds

Jeroen Verspeek, Marcos Portabella, Ad Stoffelen, Anton Verhoef

Version 4.0

25 November 2008

DOCUMENTATION CHANGE RECORD

Reference: SAF/OSI/KNMI/TEC/TN/163

Issue / Revision :	Date :	Change :	Description :
Version 0.9	2007-02-22		Draft version.
Version 1.0	2007-06-15	Major	Adapted description and figures Adapted correction tables and monitoring tables
Version 2.0	2007-10-01	Major	Adapted document to one-transponder calibrated data
Version 2.1	2007-10-22	Minor	Title changed, minor adaptations
Version 3.0	2008-03-26	Major	Adapted document to three-transponder calibrated data
Version 3.1	2008-10-01	Minor	Added section about MLE normalisation. Adaptations on figures and tables
Version 4.0	2008-11-25	Major	Adapted document to L1b version PPF6.3.0.

Summary

Based on the OSI SAF cone visualisation tools at KNMI and the CMOD5 wind sensitivity, calibration of the ASCAT scatterometer is checked. In this report we describe and evaluate normalisation corrections to the pre-operational L1b ASCAT backscatter data version PPF6.3.0 as provided by EUMETSAT based on their three transponder calibration campaign. For the left mid antenna a "wiggle" in ocean calibration results has disappeared with respect to the former version, suggesting improved L1b calibration as anticipated. In the outer swath consistent large departures remain, which need checking against other ancillary geophysical data sources to gain confidence in their validity. Indeed, still the ASCAT wind product based on L1b version 6.3.0 shows very similar characteristics to the ASCAT scatterometer wind product based on L1b version 6.2.0 and meets the wind product requirements.

Deviations between scatterometer and Numerical Weather Prediction wind derived backscatter still show a significant improvement after correction. Without correction the difference ranges from +0.5 dB to -0.4 dB going from the inner side to the outer side of the swaths. Also, the PPF 6.3.0 L1b data show smaller interbeam differences and the wiggle in the left mid beam antenna has disappeared. After the scaling correction is applied the difference ranges from -0.1 dB to +0.5 dB and is almost identical for the PPF6.3.0 and the PPF6.2.0 L1b data.

The pre-operational OSI SAF ASCAT level 2 wind product stream runs at KNMI using the pre-validated ASCAT level 1b stream at 25 km sampling as input, and may be maintained without any significant effects on product quality. The new L1b σ^0 stream will be corrected using the new linear scaling factors in the transformed z domain, which correspond to addition factors in the logarithmic domain (dB). These changes correspond to slightly resetting the ASCAT instrument gain per beam and per Wind Vector Cell (WVC) in order to maintain the backscatter data consistency and wind product quality.

In concert with EUMETSAT more detailed aspects of the ASCAT scatterometer L1b product and L2 product are currently being tested as more calibrated ASCAT products become available.

Contents

1 Introduction

A pre-operational OSI SAF ASCAT level 2 wind product stream is running at KNMI using the commissioning ASCAT L1b stream at 25 km sampling as input. The L1b σ^0 stream is corrected using linear scaling factors in the transformed z domain [STOFFELEN and ANDERSON 1997], corresponding to addition factors in the logarithmic domain (dB). These changes correspond to resetting the ASCAT instrument gain per beam and per Wind Vector Cell (WVC). The objective is set to reproduce wind distributions similar to those from the ERS scatterometer, which provides a transfer standard from the ERS to the ASCAT era.

The Advanced Scatterometer (ASCAT) [FIGA et al 2002] is part of the payload of the MetOp satellite series of which the first one, MetOp-A, has been successfully launched on 19 October 2006. ASCAT is a fan beam scatterometer with six fan beam antennae providing a swath of WVCs both to the left and right of the satellite subsatellite track. Each swath is thus illuminated by three beams and is divided into 21 WVCs of 25 km size, numbered from 1-42 from left to right across both swaths (when looking into the satellite propagation direction. [STOFFELEN and ANDERSON 1997] describe the so-called measurement space. In this space the three backscatter measurements are plotted along three axis, spanning the fore, mid and aft beam backscatter measurements. As the satellite propagates and the wind conditions on the ocean surface vary in each numbered WVC, the 3D measurement space will be filled. CMOD5 [HERSBACH et al 2007] describes the geophysical dependency of the backscatter measurements on the WVC-mean wind vector as derived from ERS scatterometer data. Since, this dependency involved two geophysical parameters, namely two orthogonal wind components (or wind speed and direction), the 3D measurement space is filled with measurements closely following a 2D surface [STOFFELEN and ANDERSON 1997]. This folded surface is conical and consists of two sheets, one sheet for when the wind vector blows against the mid beam pointing direction (upwind section) and one for an along mid beam pointing direction wind vector (downwind section). The knowledge on the position of this surface through the Geophysical Model Function, GMF, CMOD5 provides a powerful diagnostic capability for the calibration and validation of the ASCAT scatterometer, since the same geophysical dependency should apply for both the ERS and MetOp scatterometers.

Besides ocean calibration EUMETSAT relies on the rain forest response, the backscatter over ice and transponder measurements for ASCAT calibration [FIGA et al 2004]. In this report we explore ocean calibration. In this report we assume that the main challenge lies in setting the antenna pattern or gain settings of the six beams and explore normalisation corrections to the experimental L1b backscatter data as provided by EUMETSAT during the commissioning phase of MetOp.

EUMETSAT has provided several preliminary datasets during the MetOp commissioning:

1) from 19 October 2006 until 29 January 2007, denoted "ss" data;
2) from 30 January 2007 until 12 February 2007, denoted as "zz" data;
3) from 13 February 2007 until 10 October 2007. (latest configuration of the pre-validated L1b data stream denoted as "zzz" data)
4) from 10 October 2007 until 28 February 2008. One-transponder calibrated data, denoted as "PPF530" data with reference to the level 1B processor software version. This data was previously denoted as "z4" data
5) from 28 February 2008 to 23 October 2008. Three-transponder calibrated data, denoted as "PPF550".
6) from 23 October 2008 to 27 November 2008, "PPF620" data.
7) from 27 November 2008 onwards, "PPF630" data

A synchronized data set from L1b version PPF550 and PPF620 were provided by EUMETSAT. It turned out that differences in backscatter were very small, in the of the order of 0.001 dB. An update of the correction tables was not performed for this new L1b version because the differences are small compared to the radiometric and other accuracies.

A synchronized data set from L1b version PPF620 and PPF630 was provided by EUMETSAT in two batches:

Batch 1: orbit 10608 to 10648, date 2008-11-04 to 2008-11-07
Batch 2: orbit 10649 to 10702, date 2008-11-07 to 2008-11-11

In this document these synchronized data sets are used. From March 2008 onwards the L1B software identifier is written in the BUFR message and is used for automatic determination of the applicable calibration correction table in the ASCAT Wind Data Processor (AWDP).

In sections 2, 3, 4 and 5 the correction based on a visual inspection of the measurement space, the wind bias correction, the normalisation correction, and the total correction factor are described respectively. In sections 6, 7 and 8, the ocean calibration results, the wind statistics, and the Maximum Likelihood Estimator (MLE) statistics are discussed, respectively. The conclusions and outlook are presented in section 9. Note that correction tables are listed in appendix A1 and A2.

2 Visual correction

A first correction is done in order to match the cloud of ASCAT backscatter ($\sigma°$) triplets (corresponding to the fore, mid, and aft beams) to the CMOD5 geophysical model function (GMF) in the 3-D measurement space [HERSBACH et al, 2006]. We use the OSI SAF visualisation package [VERSPEEK 2006-2] to produce the plots in z-space, i.e., (z_{fore}, $z_{aft,}$ z_{mid}) where $z=(\sigma°)^{0.625}$ [STOFFELEN, 1998]. Figure 1 is an example of such a visualisation from ASCAT. The double cone surface of CMOD5 is depicted in blue. The measured data is shown as a cloud of black points around the cone surface
.
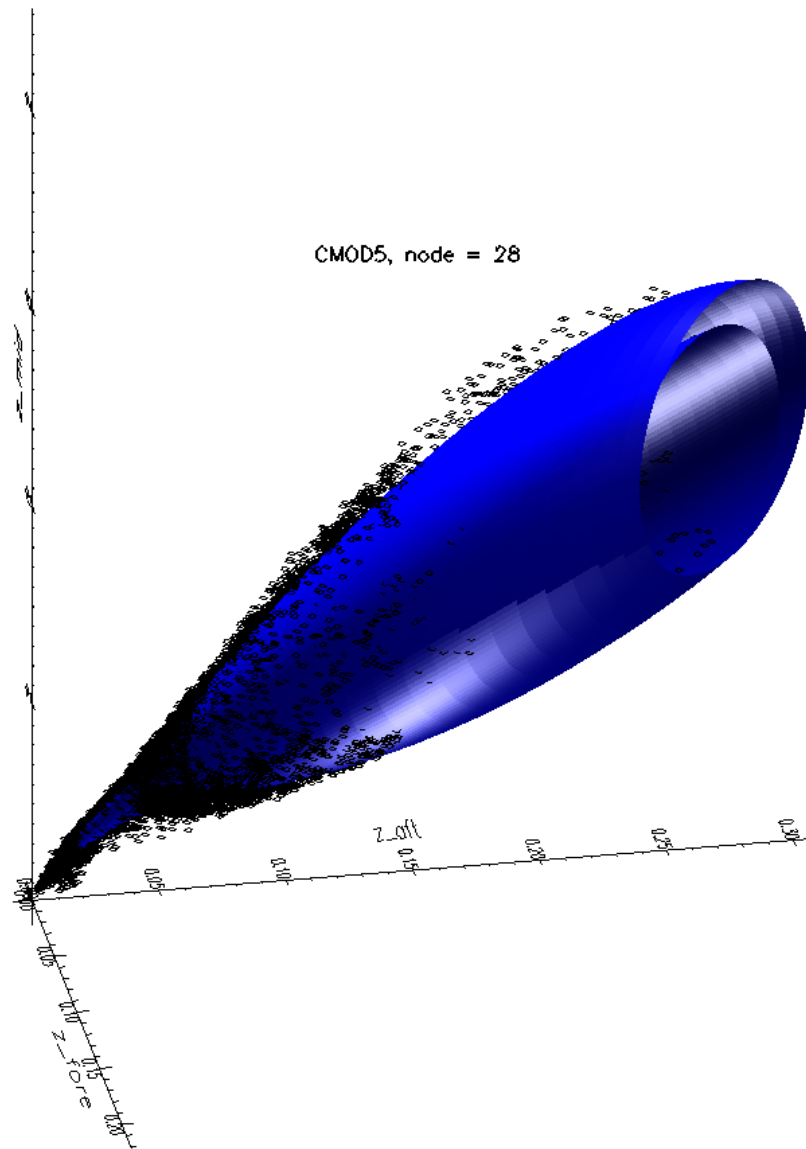
Figure 1 – CMOD5 wind cone with measured data points for WVC 28.

By looking at the projection of the wind cone on and data points in the proximity of the plane $z_{fore} = z_{aft}$, a normalisation factor for the mid beam is determined such that the CMOD5 cone by approximation fits the measurement points for each WVC. In the same way, by looking at a plot of the z_{fore} versus z_{aft} measurement points and the projection of the CMOD5 cone on the plane $z_{mid} = 0$, correction factors for the fore and aft beam are determined, such that the measurement points are distributed symmetrically. As such, the normalisation factors for the fore and aft beam are coupled in the following way:

$$z^{corr}_{fore} = 1/z^{corr}_{aft}$$

Equation 1

This deformation has the effect that the cloud of data points becomes symmetric, but does not correct correlated fore and aft beam biases. The normalisation factors are determined per wind vector cell (WVC).

Figure 2 shows the visualisation plots ($z_{fore}=z_{aft}$) for WVC 42 , i.e., the outer WVC of the right swath. Green points belong to the downwind sheet of the GMF cone surface, while purple points belong to the upwind sheet of the GMF surface. The retrieved wind is the wind solution that has a wind direction that is closest to the collocated NWP wind obtained from ECMWF. Figure 2a) shows

7

uncorrected data from the original normalisation table (ss) and Figure 2b) shows the visual corrected data. Figure 2a) shows a clear discrepancy between data points and GMF, which is much improved in Figure 2b).

a)   b)
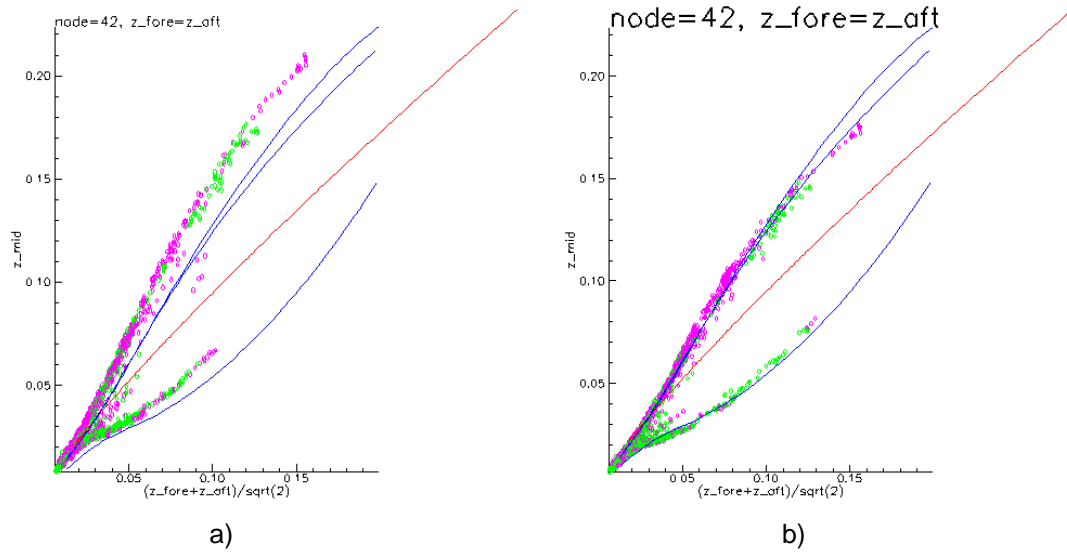
Figure 2 – CMOD5 wind cone (blue) and ice line (red) on the plane $z_{fore}=z_{aft}$, data points with 1 dB tolerance on either side of the plane.
a) ss normalisation table, uncorrected data
b) ss normalisation table, visual corrected data

Figure 3 shows the visualisation plots (projection on plane $z_{mid}=0$) for WVC 42. In Figure 3a) (uncorrected) the cloud of data points shows an asymmetry between z_{fore} and z_{aft}. The cloud seems to be rotated around the z_{mid} axis. Figure 3b) (visual corrected data) shows a more symmetrical distribution of data points with respect to the GMF.

a)   b)
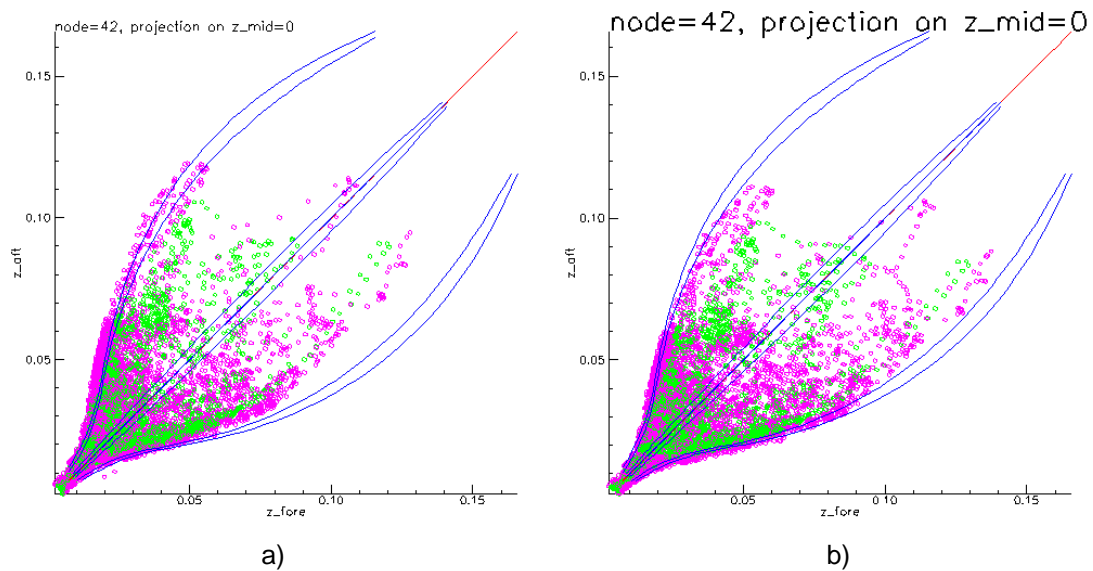
Figure 3 – Projection of the CMOD5 wind cone (blue), ice line (red) and data points on the plane $z_{mid}=0$
a) ss normalisation table, uncorrected data
b) ss normalisation table, visual corrected data

Note that the distribution of measurement points in figures 1-3 depends on:
- Kp noise;
- Beam collocation noise due to wind variability [PORTABELLA and STOFFELEN, 2006];
- The true underlying wind vector distribution that, for example, is far from uniform in wind direction.

It should be mentioned that all corrections are applied to the level 1b data before inversion with CMOD5.5 and ambiguity removal takes place in the level 2 processing. Thus the corrections will have influence on the quality control of each measured triplet.

3 Wind speed bias correction

After balancing the fore and aft beam for cone symmetry and bringing the mid beam measurements in line with the CMOD5 values on the cone, one degree of freedom remains in the normalisation of the cone. This degree of freedom lies in the translation of the cone along its major axis. Its first order effect is a wind speed bias after CMOD5 inversion, while effects on the misfit of the measurement triplets with respect to the cone surface are mainly second order. Therefore, a second normalisation is applied to correct for the remaining wind speed bias on top of the visual normalisation.

First the relative wind sensitivity is determined. It is defined as $(1/z)*(dz/dV)$ and is taken at $V_0 = 8$ m/s because this gives a good approximation of the modal value, both for the wind speed and for the CMOD5 dz/dV derivative.

The z value is determined as an average over the CMOD5 upwind ($\Phi = 0°$), downwind ($\Phi = 180°$) and the two crosswind values ($\Phi = 90°$ and $\Phi = 270°$). Since CMOD5 is a second order harmonic in z space this provides the B_0 value. The derivative of z with respect to V, dz/dV is calculated using the central derivative approximation:

$$z_{ave}(\theta, V) = \frac{1}{4} \sum_{n=0}^{3} z(\theta, V, \phi_n), \phi_n = 90^0 \cdot n$$

<div align="right">**Equation 2**</div>

$$(dz/dV)_{V=V_0} = \frac{z_{ave}(\theta, V_0 + h) + z_{ave}(\theta, V_0 - h)}{2h}$$

<div align="right">**Equation 3**</div>

with $h = 0.1$ m/s. The wind speed bias is the difference between the retrieved wind and the first guess ECMWF NWP wind. This bias is multiplied with the relative wind sensitivity to get the wind bias normalisation factors. The correction factors are determined per WVC and per beam. See appendix A2 for tables related to the wind speed bias correction factors.

First guess ECMWF NWP winds are used as reference at this point, since the more precise triple collocation cal/val procedures require a year's worth of data, while only a limited set of ASCAT data has been available. ECMWF [HERSBACH, personal communication] reports that their routine operational comparison with buoys indicates that earlier low biases in the ECMWF winds have disappeared over recent time with the implementation of new ECMWF IFS model cycles.

CMOD5 winds were also found to be biased low [HERSBACH et al, 2007, PORTABELLA and STOFFELEN, 2007]. As such, all CMOD5 winds were corrected here to become 0.5 m/s stronger.

Figure 4 and Figure 5 show the same as Figure 2b and Figure 3b, respectively, but with the wind speed bias correction added to the visual correction. Note that the wind speed bias corrected data

points (Figure 4 and Figure 5) are stretched away from the origin towards higher CMOD5 wind speed values as compared to the only visually corrected data points (Figure 2b and Figure 3b).
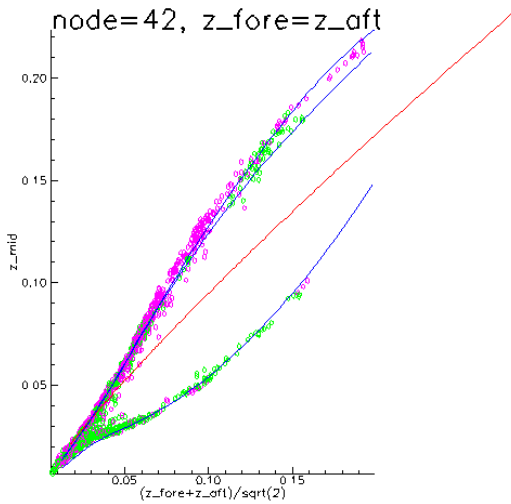
Figure 4 - Same as Figure 2b, but with the wind speed bias correction also applied.
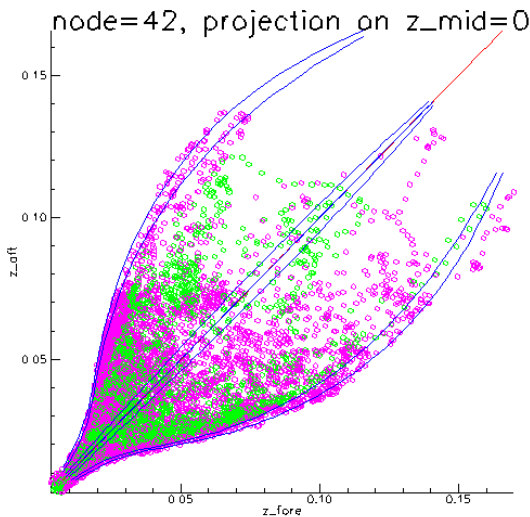
Figure 5 -Same as Figure 3b, but with the wind speed bias correction also applied.

4 Normalisation correction

The visualisation and wind speed bias corrections were applied to adapt the backscatter values in the original (version ss) L1b stream. Later on, EUMETSAT several times improved their normalisation tables in the L1b processing. The normalisation factors are assumed to be multiplication factors in linear space, like the visual correction that we apply. Because all correction factors are linear, the corrections can be applied on top of each other. Normalisation correction tables are determined for each update of the L1b data. This is done by averaging the σ^0 differences in dB value from the new L1b data stream and the parallel original L1b data steam over one or more collocated orbits. The differences appear rather constant and show insignificant spread, confirming that the main effect in these conversions is a gain factor. Figure 6a) shows the average

value per antenna and WVC of the difference in σ^0 value between the PPF630 and the PPF620 data stream. Figure 6b) shows the standard deviation (SD) for the correction as shown in Figure 6a). Synchronized batches are used for an assessment of the spread in the differences (SD). The differences show a smooth course. The SD plots show small values indicating that the pattern is persistent. It is an order of magnitude below the typical calibration changes. This is compatible with all earlier ASCAT calibration changes, thus guaranteeing a constant-quality backscatter input to the L2 processing.

a)   b)
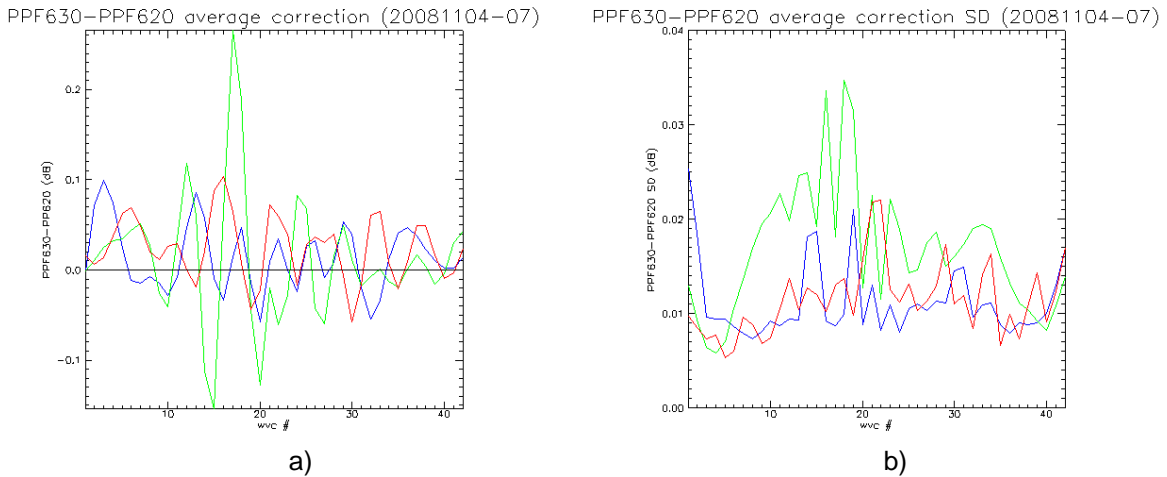
Figure 6 – Average difference and standard deviation of the difference between the L1b versions PPF630 and PPF620 (2008-11-04 / 2008-11-07) for the fore (red), mid (green) and aft (blue) antenna per WVC.
a) average σ^0 difference
b) standard deviation of the difference

Figure 7a) shows the backscatter difference for the mid antenna from the ascending part of the orbits on 2008-11-05. Figure 7b) shows a detail of the map in Figure 7a). Figure 7c) and Figure 7d) show the same data corrected for the average PPF630-PPF620 σ^0 difference as shown in Figure 6a). Any dependency of the difference in backscatter on geographical location should be visible in these figures. The dependency appears to be mainly on WVC number or incidence angle. The orbits have a systematic pattern across the swath, showing the WVC dependency of the correction. In Figure 7c) there seems to be a dependency on latitude, but the differences are very small, smaller than 0.05dB in absolute value, slightly positive (blue) on the Northern hemisphere, and slightly negative (green) on the Southern hemisphere. The other beams and calibration changes show similar corrections and SDs.

a)   b)

c)   d)
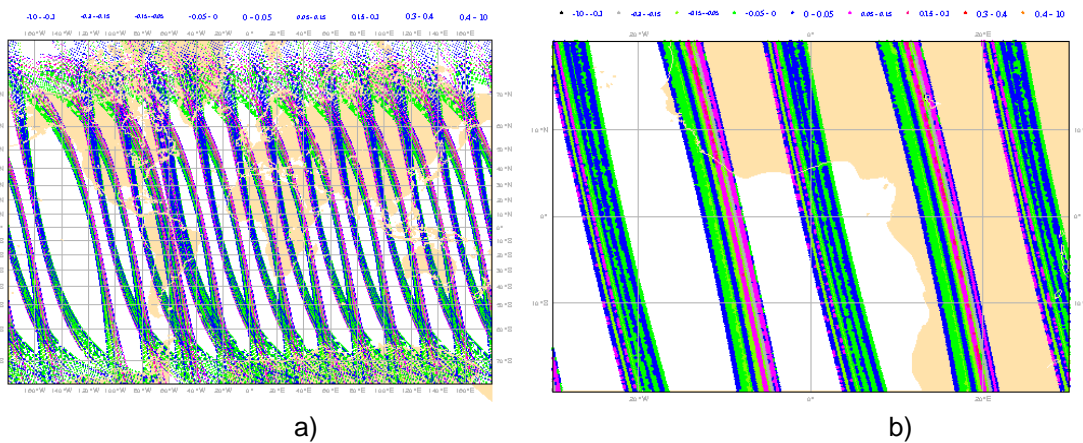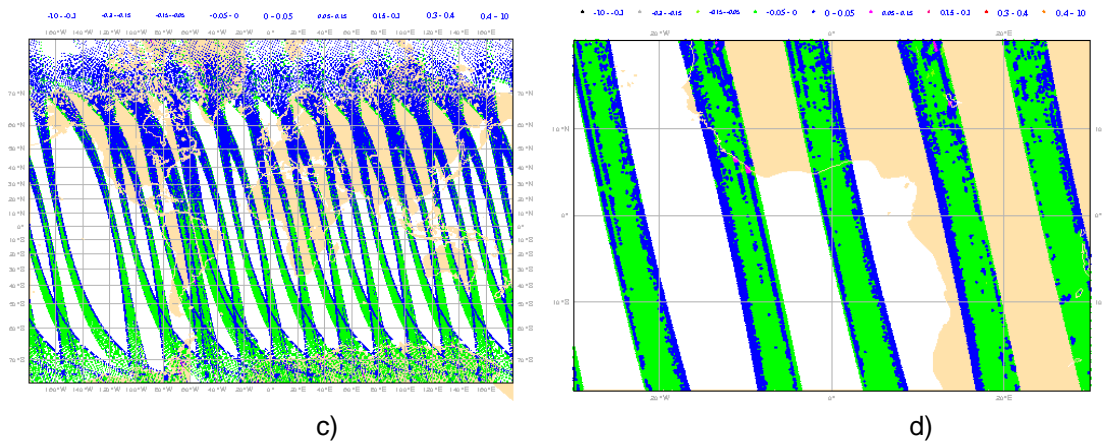
Figure 7 – Spatial plot of the average difference in σ^0 of the PPF630-PPF620 data for the mid antenna . Data from the ascending part of the data from 2008-11-05 is used.
a) Global plot
b) Detail plot (West-Africa)
c) Global plot, deviations from the average values from figure Figure 6a)
d) Detail plot (West-Africa), deviations from the average values from figure Figure 6a)

5 Total correction factors

A total correction is applied to adapt the backscatter values in the level 1b stream, which consists of the visualisation correction, the wind speed bias correction, and the normalization correction as discussed in sections 2, 3 and 4. In the following sections GMF version CMOD5.n is used in the ASCAT Wind Data Processor (AWDP) and the ocean calibration. CMOD5.n is a version of CMOD5 that is adapted for neutral winds. It is basically identical to CMOD5 with a 0.7 m/s shift in the input wind speed. The shape of the wind cone for CMOD5 and CMOD5.n is identical. The 28 fit-coefficients in the CMOD function have been recalculated for CMOD5.n by ECMWF, which lead to negligible deviations within the numerical precision of the fit procedure. The neutral wind speed GMF is the result of a triple collocation study with ECMWF winds and buoy winds [Portabella and Stoffelen 2007].

Figure 8a) shows CMOD5.n and the uncorrected PPF630 data for the plane $z_{fore} = z_{aft}$. Figure 8b) shows the same data after the total correction has been applied. The PPF630-data are transformed back to ss-data using the normalisation correction, and then the visualisation and wind speed bias corrections are applied. Figure 9 shows the same as Figure 8 but now for the projection of the wind cone and data points on the plane $z_{mid} = 0$. Figure 10 shows the intersection of the cone with the plane $z_{fore} + z_{aft} = 2z_{ref}$, for several values of z_{ref}, which correspond to (approximately) constant wind speed values. Also here the match between measurements and GMF is good. For other WVCs similar plots have been examined (not shown). For all examined WVCs the correspondence between data and model remains good.

12

a)   b)
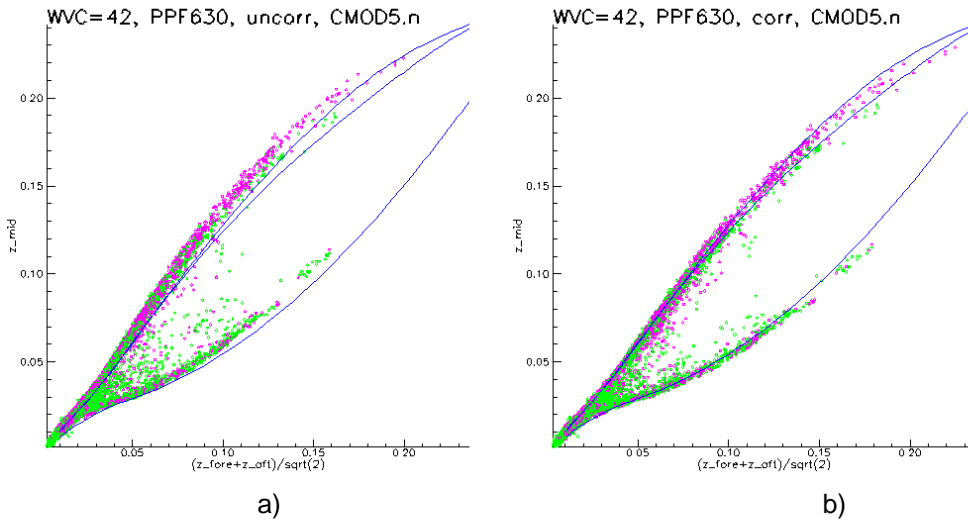
Figure 8 - Projection of the CMOD5.n wind cone (blue) and data points (green and purple) on the plane z_{fore} = $z_{aft.}$.
a) PPF630 uncorrected data
b) PPF630 with KNMI total correction applied

a)   b)
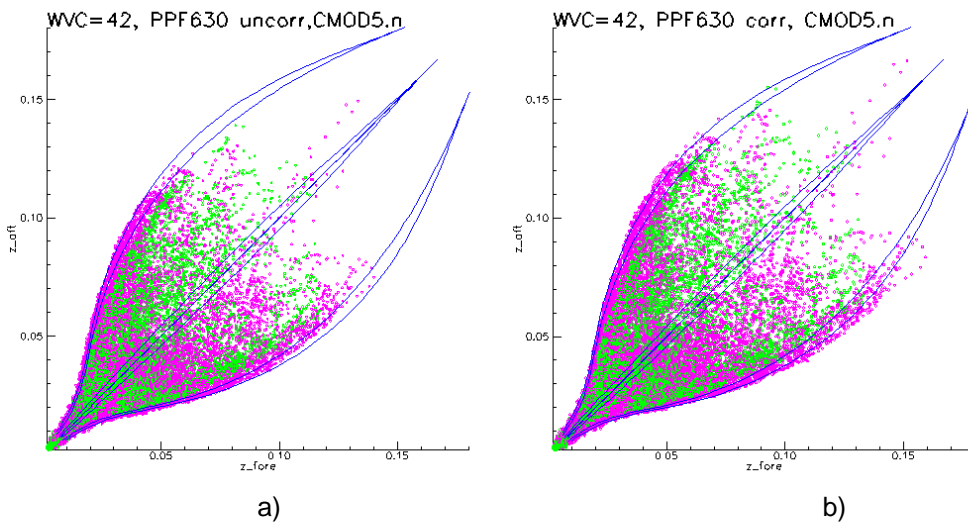
Figure 9- Projection of the CMOD5.n wind cone (blue) and data points (green and purple) on the plane z_{mid} = 0.
a) PPF630 uncorrected data
b) PPF630 with KNMI total correction applied

13
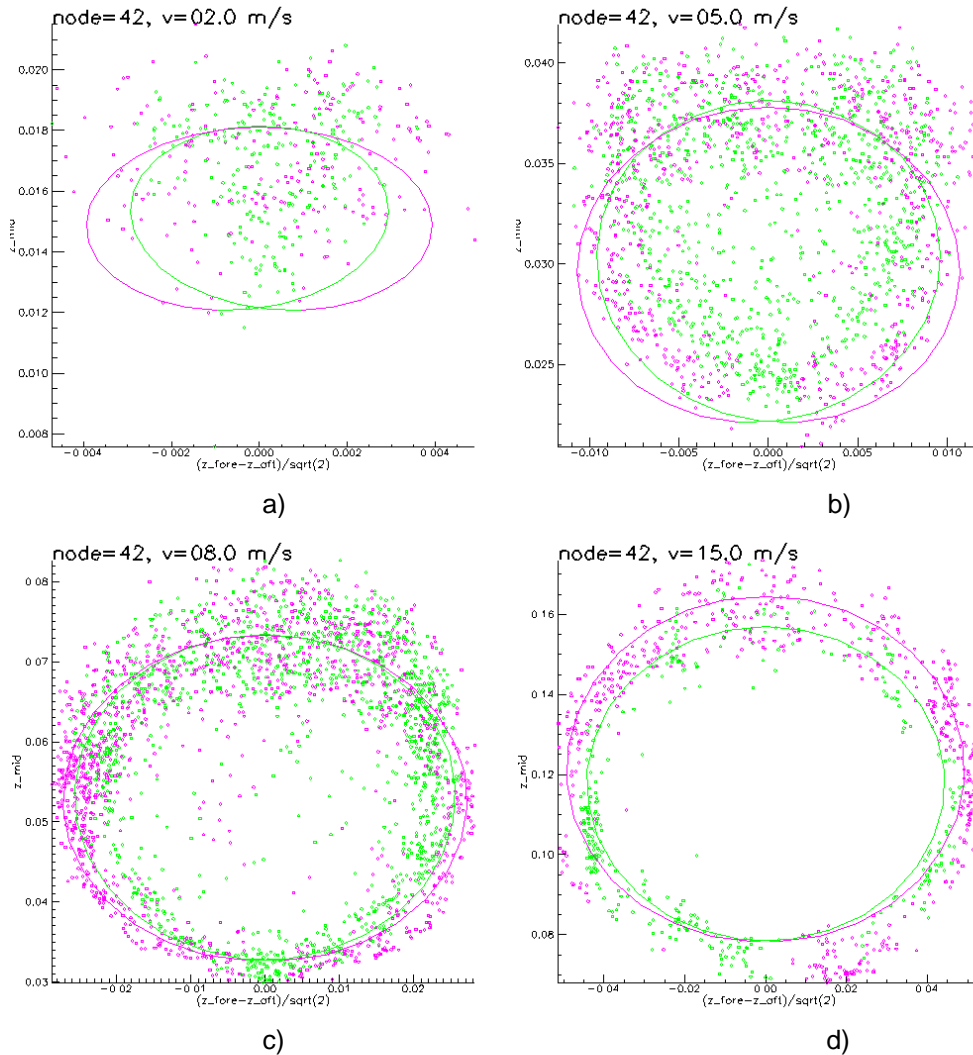
Figure 10 – Visualisation for WVC 42 of the corrected σ^0 triplets (version PPF6.3.0) and CMOD5.n (coloured ellipses), for several intersections of the cone with the plane $z_{fore} + z_{aft} = 2z_{ref.}$, corresponding to the following wind speeds:
a) V = 2 m/s b) V = 5 m/s c) V = 8 m/s d) V = 15 m/s

The correction factors are again determined per wind vector cell (WVC) and beam. See appendix A1 for the normalisation correction factor table.

Figure 11a) and b) show the total correction factor for the PPF620 and PPF630 data respectively. The correction from Figure 6a) has been added to the total correction factor for the PPF620 data in order to generate the total correction factors for the PPF630 data. The patterns look very consistent for all antennas. This is an indication that the inter-beam biases are small and that only an overall correction, which is basically incidence angle dependent, is needed. The corrections for PPF630 look even more consistent than for PPF620, the wiggle in the left mid beam antenna response has disappeared. For high incidence angles the correction is still large, i.e., above 1 dB. This may be caused by either a L1b calibration issue or a CMOD5.n issue, since CMOD5.n has not yet been validated for such high incidence angles. We suggest ancillary sea ice, rain forest and soil geophysical comparisons to gain confidence in the backscatter calibration in the outer swath..

14

a)   b)
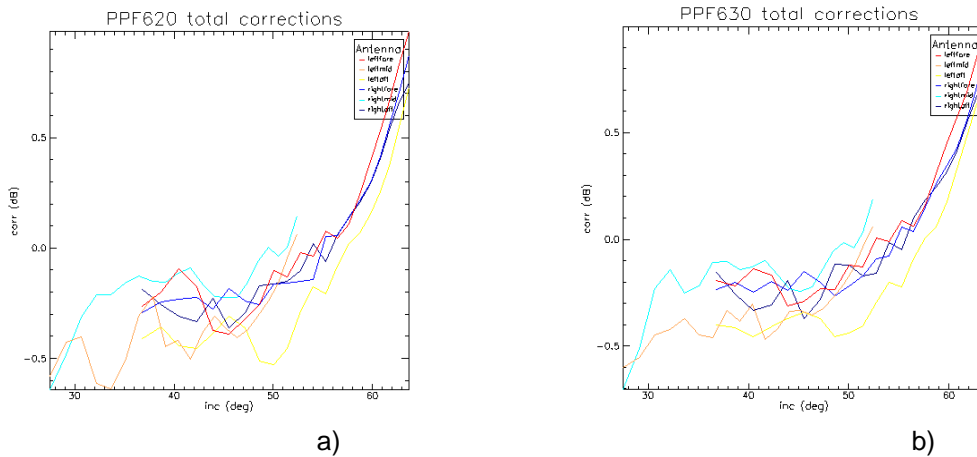
Figure 11 – Total correction factors per antenna and incidence angle
a) PPF620 data
b) PPF630 data

The tables with total correction factors can be found in appendix A2.

6 NWP backscatter comparison

A NWP simulated backscatter comparison [VERSPEEK 2006] is performed with the parallel L1b data steams PPF620 and PPF630, both for the corrected and uncorrected case. Both L1b products are processed with AWDP using 2D-VAR ambiguity removal to provide a level 2 product with scatterometer retrieved winds and collocated NWP winds from the ECWMF model. The data is conservatively filtered to exclude land and ice.

Figure 12 shows the results. Figure 12a) and Figure 12b) show the PPF620 and PPF630 uncorrected case where the difference between the measured averaged σ^0 values and the averaged σ^0 values simulated from the NWP winds is depicted. The difference ranges from +0.6 dB for to inner side to -0.4 dB for the outer side of the swath in Figure 12a) and Figure 12b). Furthermore, the difference shows a systematic trend which tends to large negative values for all antennae. The interbeam bias is improved for the PPF630 case with respect to the PPF620 case, showing less difference between the antennas. Most notably the left mid beam response "wiggle" has disappeared.

a)   b)

c)   d)
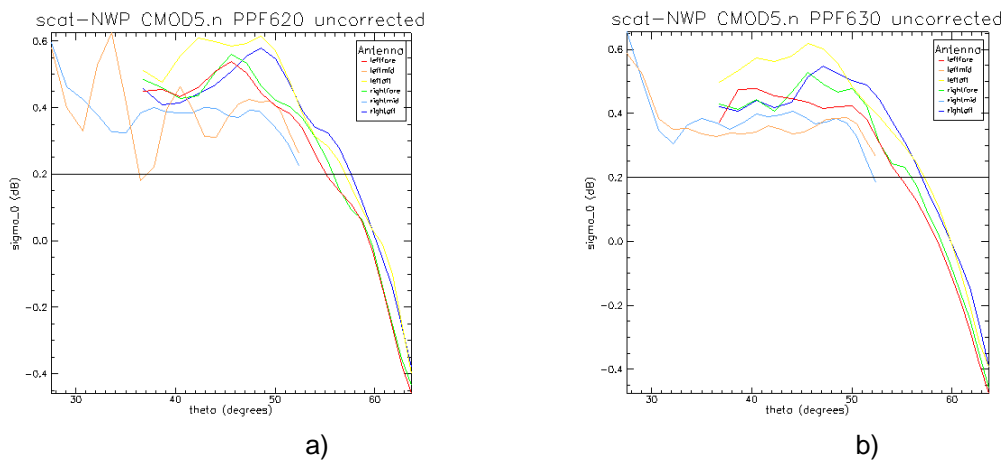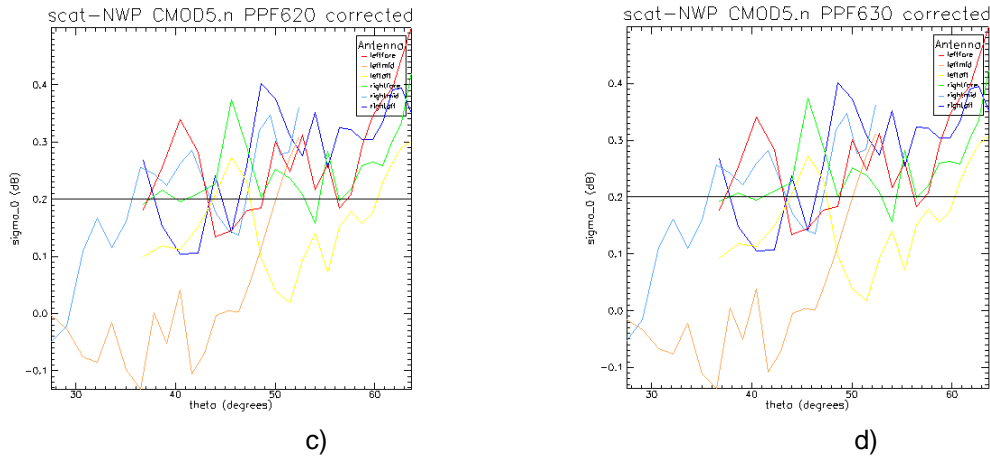
Figure 12 – NWP comparison results for the data from 2008-11-04. to 2008-11-07 of CMOD5.n backscatter values based on real ECMWF 10m winds with
a) PPF620 data (uncorrected)
b) PPF630 data (uncorrected)
c) PPF620 data (corrected)
d) PPF630 data (corrected)

For Figure 12c) and Figure 12d) the correction factors were applied to the L1b backscatter values. The difference ranges from -0.1 dB to +0.5 dB. This is a clear improvement with respect to the uncorrected cases. The σ^0 bias is in both cases around +0.2 dB. This corresponds to the fact that we use real 10-m ECMWF winds as input for CMOD5.n. When CMOD5.5 would have been used instead of CMOD5.n the bias would be 0.2 dB lower, so around zero. There is little systematic behaviour in the σ^0 bias. Only a slight increase with the incidence angle remains.

7 Wind statistics

In this section some statistical plots comparing ASCAT wind and ECMWF wind are given.

First of all it is of interest to look at differences between the PPF630 corrected and PPF620 corrected wind solutions. Because the PPF630 correction incorporates the average difference between PPF630 and PPF620, both wind solutions are expected to highly correlate and show only small differences. Figure 13a) shows a scatter plot of the wind vector differences for the two data streams for one orbit. The outliers can be clearly identified and are due to selection of the "other" solution by 2DVAR ambiguity removal at low winds. The number of outliers is in the order of a fraction of 0.001 of the total number. Figure 13b) shows the same plot but in a zoomed view. The points are centred around the origin with a standard deviation of 0.23 m/s in u and v direction.

16

a)   b)
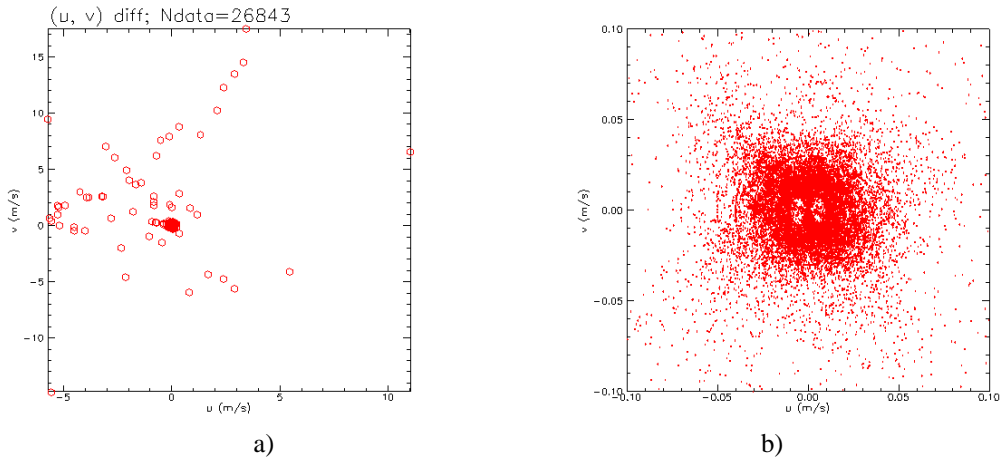
Figure 13 – Scatter plot of the wind vector difference of PPF630 corrected and PPF620 corrected solutions for one orbit of data.
a) wide view b) zoomed view

Figure 14 and Figure 15 show the wind statistics per WVC for PPF630 and PPF620 respectively.

Corrected data is represented in red, uncorrected data in orange. The statistics for the corrected data sets PPF630 and PPF620 are almost identical. This is to be expected because the PPF630-to-PPF620 correction is small and almost linear. The wind speed bias shown in Figure 15a) has an average value of 0.2 m/s for the corrected case. This is due to the fact that CMOD5.n is used while we compare to real ECMWF winds rather than to neutral winds. Neutral winds have a bias of 0.2 m/s with respect to real 10m winds.

For the uncorrected cases, already significant bias appears in WVCs in the projected ERS swath. The underscaled winds from the uncorrected set result in smaller wind speed SD in the outer swath, and a larger wind direction SD than for the corrected set.

a)   b)

c)

d)
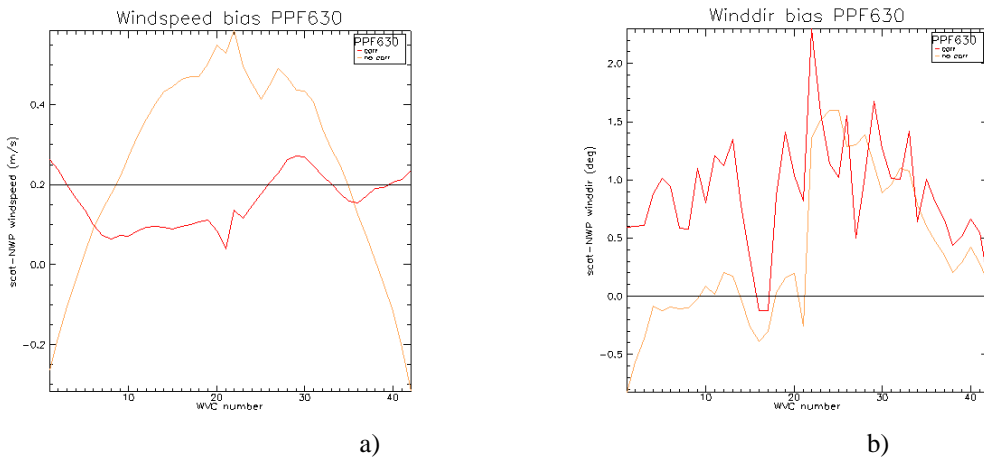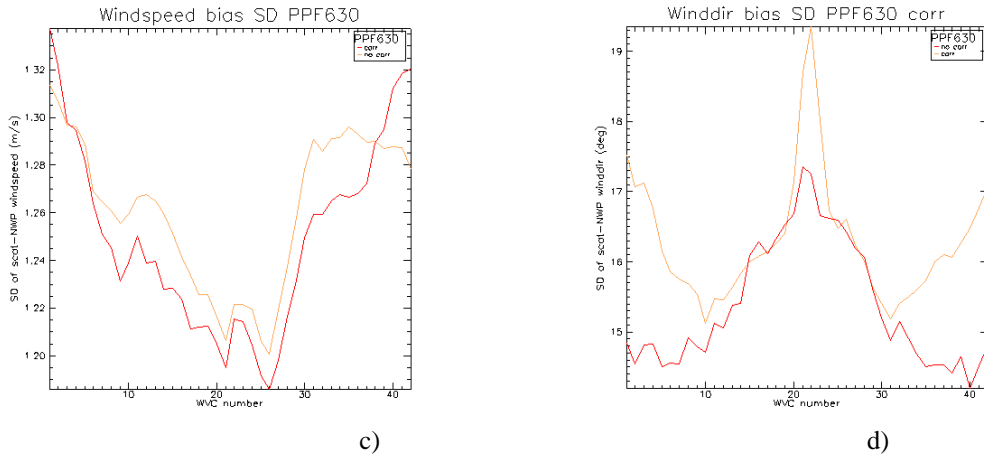
Figure 14 – Wind comparison per WVC between ASCAT and ECMWF for 2008-11-04 / 2008-11-07, PPF630 corrected and uncorrected. Wind direction statistics are for the 2DVAR wind solutions for ECMWF winds larger than 4 m/s.
a) wind speed bias b) wind direction bias
c) wind speed SD   d) wind direction SD.

a)

b)

c)

d)
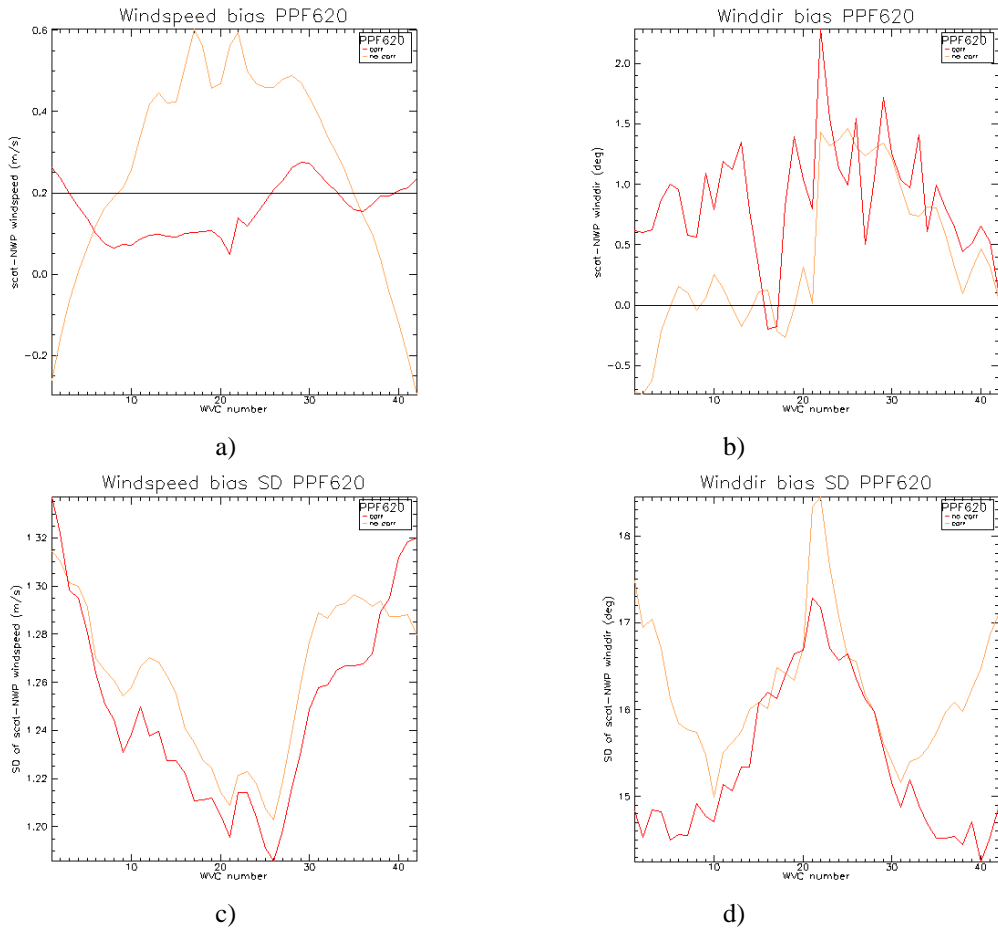
Figure 15 – Wind comparison per WVC between ASCAT and ECMWF for 2008-11-04 / 2008-11-07, PPF620 corrected and uncorrected. Wind direction statistics are for the 2DVAR wind solutions for ECMWF winds larger than 4 m/s.
a) wind speed bias b) wind direction bias
c) wind speed SD   d) wind direction SD.

Figure 16 and Figure 17 show the wind scatter plots for corrected PPF630 and PPF620 data respectively. Only insignificant differences appear in the wind speed contour plots and the wind direction contour plots for ECMWF winds above 4 m/s. The corrected PPF630 and PPF620 data sets are statistically very similar in terms of wind performance, as may be expected from Figure 13.

N=1131867
mx=7.782085 my= 7.624901
cor_xy= 0.93008214

a)

N=978818
mx=167.972046 my=168.882111

b)

N=1131867
mx= -0.628135 my= -0.498089
cor_xy= 0.97568554

c)

N=1131867
 mx=0.271371 my=0.248876
cor_xy= 0.9497917

d)
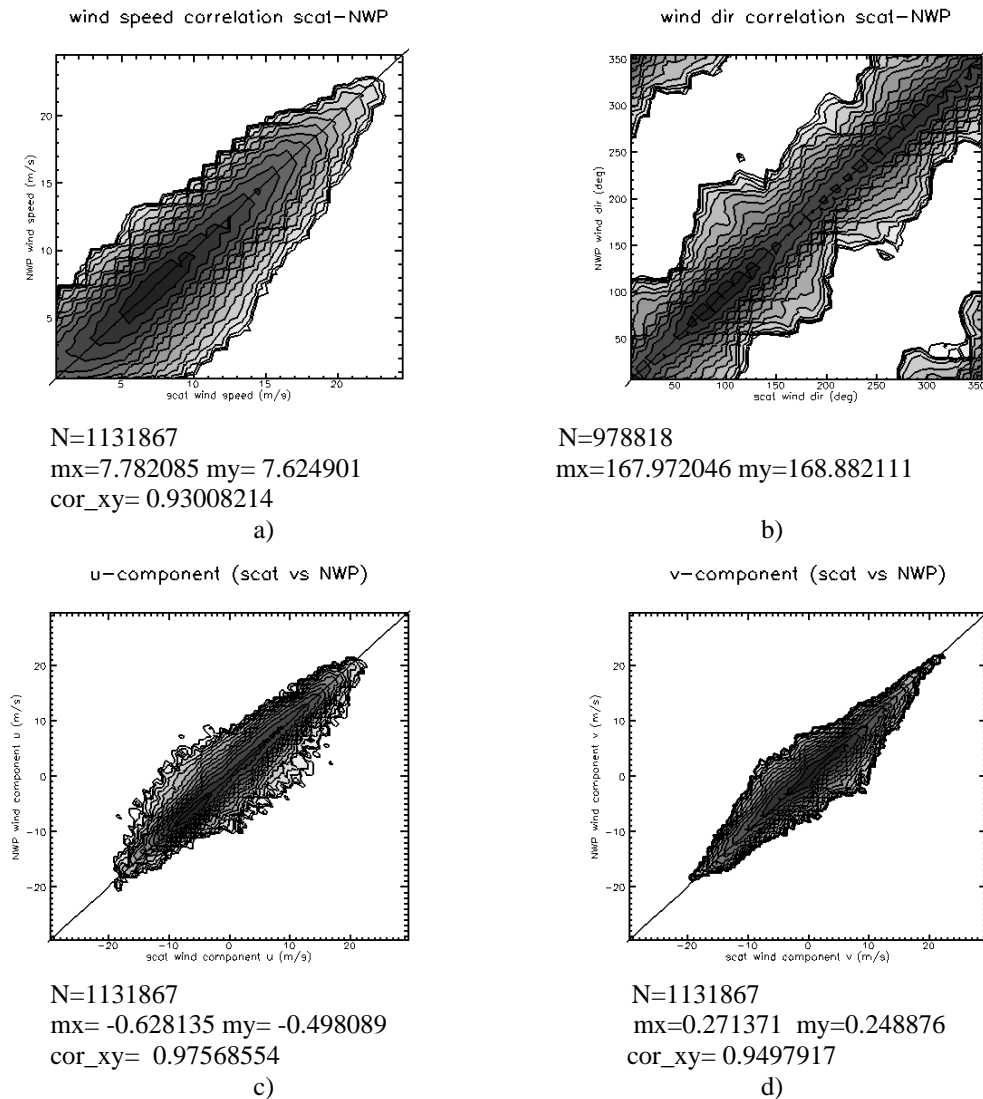
Figure 16 – Two-dimensional histogram of the 2D-VAR KNMI-retrieved wind solution versus ECMWF wind for all WVCs. The PPF630 data after OSI SAF correction is used. N is the number of data; mx and my are the mean values along the x and y axis, respectively; and cor_xy is the correlation coefficient for the xy distribution. The contour lines are in logarithmic scale: each level up is a factor of 2. Lowest level=10, there are 15 levels in total.
a) wind speed (bins of 0.4 m/s) b) wind direction (bins of 2.5°) for ECMWF winds larger than 4 m/s.
c) wind component u (bins of 0.4 m/s) b) wind component v (bins of 0.4 m/s)

N= 1131881
mx=7.782948 my= 7.624891
cor_xy= 0.9301694

a)

N= 978830
 mx= 167.956192 my= 168.881744

b)

N= 1131881
mx=-0.625862 my= -0.498122
cor_xy= 0.9756745

c)

N= 1131881
mx= 0.270251 my= 0.248925
cor_xy= 0.94983774

d)
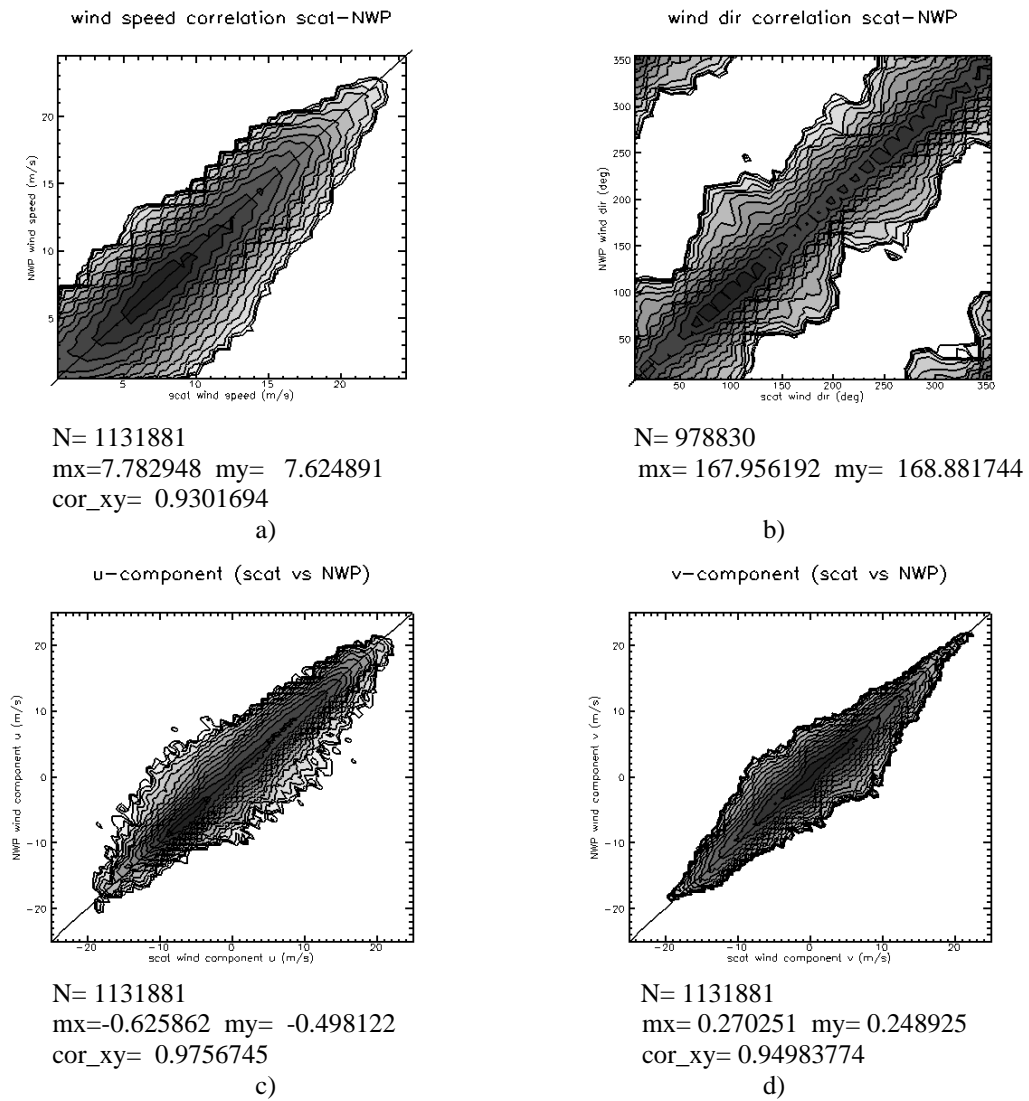
Figure 17 – Same as Figure 16 but now for the PPF620 data (corrected).

8 MLE statistics and normalisation

Figure 18 shows the normalised distance to cone or Maximum Likelihood Estimator (MLE) [PORTABELLA and STOFFELEN 2006] as a function of WVC for the PPF630 corrected and uncorrected cases. It is clear that the corrected case shows larger accumulations at the origin, i.e., triplets are closer to the CMOD5 cone, as compared to the uncorrected. Furthermore the uncorrected case shows a clear systematic error. For the outermost WVCs the MLE shows more negative values, corresponding to points outside the cone. In the corrected case Figure 18b) these systematic errors are not present anymore.
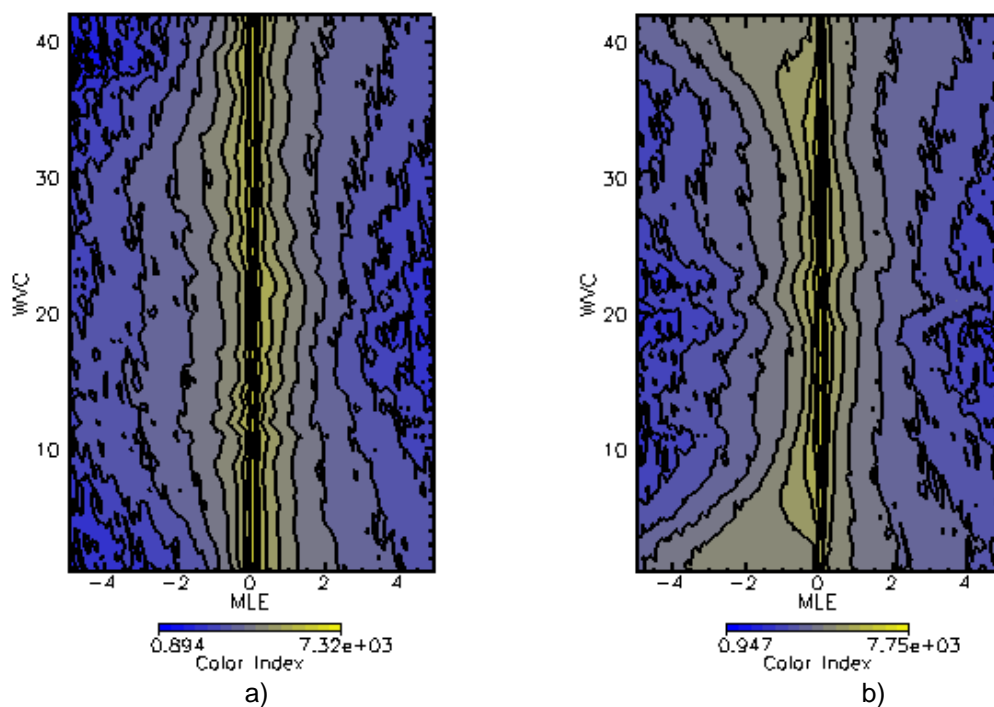
Figure 18 - MLE distribution per WVC shown. The data range is divided into 15 levels equally spaced on a log2 scale, each successive level is a factor of 2 higher than the previous level.
a) PPF630 corrected b) PPF630 uncorrected

Figure 19 shows the MLE as a function of the scatterometer wind speed for the PPF630 corrected and uncorrected cases. For high wind speed values the cone cross section is large compared to the spread of the triplets around the cone surface. A symmetrical pattern around the origin is expected here as an equal amount of triplets are on the inner and outer side of the cone surface (see Figure 10). For low wind speed values, i.e. smaller than ~4 m/s, the cone radius is small and the spread of triplets is relatively large. More triplets are expected to lie outside the cone and thus have a negative MLE. The visual correction moves the points on average towards more positive MLE values.

a)
b)

Figure 19 – Cone distance distribution versus measured wind speed
a) PPF630 corrected b) PPF630 uncorrected

Note that around 5 m/s most corrected triplets lie within the cone. This corresponds to earlier assessments that the CMOD5 cone is too wide for these winds [Portabella and Stoffelen, 2006]. After the ASCAT Cal/Val, we anticipate to use the MLE to correct CMOD5.n.

Routine monitoring statistics are accessible through the OSI SAF ASCAT product viewer web site: http://www.knmi.nl/scatterometer/ascat_osi_25_prod/ascat_app.cgi by selecting "Monitoring information".

The MLEs in the ASCAT BUFR product have been normalised. In order to compute a normalisation table, ASCAT 25-km data from 20 September 2008 to 19 October 2008 (both inclusive) have been reprocessed. In the wind inversion, the CMOD5.n GMF for neutral winds was used [VERHOEF et al 2008] and the appropriate backscatter correction (PPF630) was applied. All WVCs with latitude above 55 degrees North or below 55 degrees South were skipped to exclude any ice contamination. Only those wind solutions closest to the ECMWF forecast winds and with wind speeds above 4 m/s have been used. No quality control regarding maximum acceptable MLE values was applied. Using these data, for each WVC number (1 to 42), the mean absolute cone distance was calculated: <MLE1>.

The reprocessing was repeated, but in this second step the MLEs were normalised using the <MLE1> table obtained in the first step. Moreover, WVCs with an absolute normalised MLE above 18.45 were skipped, yielding a rejection rate of approximately 0.4 to 0.5%. For the accepted data, the mean absolute cone distance vs. WVC number was calculated again: <MLE2>. The final MLE normalisation table was computed as the product of the mean values from step 1 and 2 WVC-by-WVC: <MLE> = <MLE1> <MLE2>. Also, a quality control threshold table QC (again as a function of WVC number) was computed as QC = 18.45 / <MLE2>. WVCs with a normalised absolute MLE value above the QC table value are rejected in the wind processing software. In this way, we keep the rejection rate at 0.4 to 0.5%.

The justification for the MLE threshold of 18.45 is that we looked for a value that produced a rejection rate of about 0.4%, which was the initial rejection rate of the AWDP ASCAT quality control before any development or tuning. The reason for this is that we discovered that users were very satisfied with such a low rejection rate, as compared to the rejection rate of 1-2% that was obtained in the ERS processing in the past. Actually we see that there is no sharp cut in the MLE (with respect to the quality of the data) but rather a smooth degradation of the quality of the winds as the MLE increases.

Using the MLE normalisation table that we thus obtained for wind speeds above 4 m/s, i.e. <MLE>, we also looked at the MLE characteristics as a function of wind speed and WVC number for low wind speeds. It appears that the MLEs strongly increase below 2 m/s. This also leads to a strong increase of the rejection rate at low wind speeds, which is generally undesirable: for wind speeds below 2 m/s, the wind speed and wind component deviations from the true wind are almost always small and well within the product specification. Hence we decided to apply an extra normalisation to the MLEs below 2 m/s. A wind speed dependent parabolic function (not shown) was fitted to the mean MLEs below 2 m/s and this function is used as an extra (WVC independent) correction value for the MLEs.

Figure 20 shows the final results after applying the <MLE> normalisation and using the QC threshold. The mean MLEs of the wind solutions closest to the ECMWF background winds are close to 1 as expected from the performed normalisation. The mean MLE is not exactly equal to 1 since in this plot also low winds (for which an ad-hoc normalisation using the parabolic function is performed) are taken into account. The mean MLE of the first rank solutions is around 0.8 and reasonably constant over the swath. The rejection rate increases from ~0.1% to ~0.7% when we go from the inner part to the outer part of the swath. This can be explained as follows. The cone opens up with incidence angle. Therefore, larger MLE values inside the cone are more frequent in the outer swath (less aliasing effect). Also noise is larger at higher incidence angle. This effect broadens the MLE distribution at high incidence angles and therefore increases the QC rejection rate.
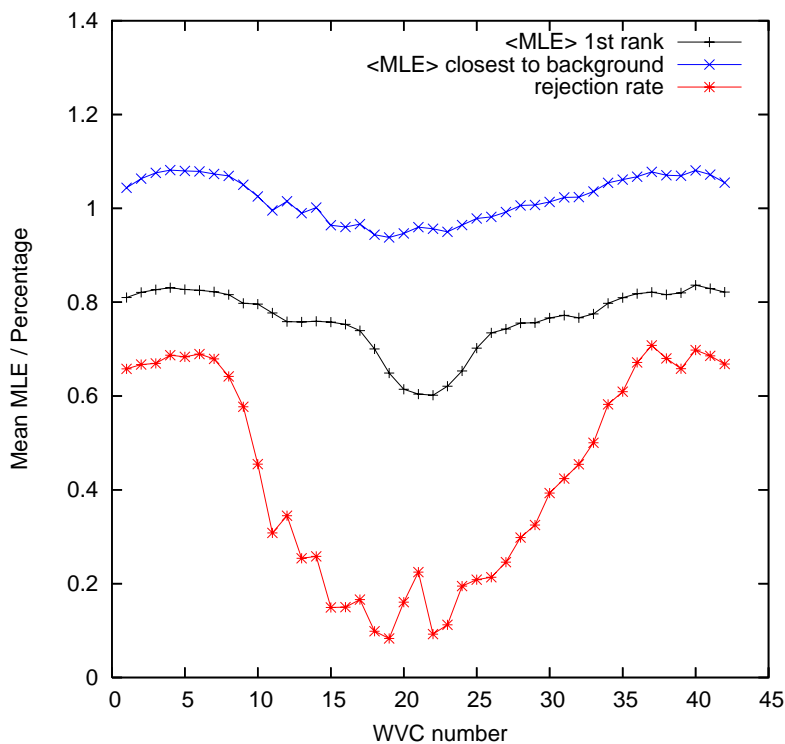
Figure 20 – ASCAT mean MLE (accepted wind solutions) of the first rank and closest to background wind solutions and rejection rate (%) as a function of WVC number. Results are shown for all wind speeds, including those below 4 m/s.

9 Conclusions

Based on the OSI SAF cone visualisation tools at KNMI and the CMOD5 wind sensitivity improved calibration of the ASCAT scatterometer is attempted. CMOD5 was carefully derived for the ERS scatterometer and thus our calibration should result in the compatibility of the ERS and ASCAT scatterometer products. Indeed, the scatterometer wind product of ASCAT is shown to have similar characteristics to the ERS scatterometer wind product and meets the wind product requirements.

ECMWF short range forecast winds are used here as reference. With the implementation of new ECMWF model cycles the ECMWF winds may become more or less biased. ECMWF verification statistics indicate that the low bias of ECMWF winds at the beginning of this century (e.g. [HERSBACH et al 2007]) have compensated by more recent ECMWF model cycles [HERSBACH, personal communication). Moreover, the random wind component errors in ECMWF and ERS scatterometer winds and their respective spatial representation are generally different. These differences may result in absolute overall biases of a few 10th of a m/s; which results in a few 10th of dB uncertainties in backscatter as well, however, rather uniformly spread over the WVCs [STOFFELEN 1999].

The ASCAT PPF630 L1b backscatter data, is compared to the currently used PPF620 L1b backscatter data. For the corrected case, consistency between the two sets is found, and the new "PPF630" set shows smaller interbeam differences, and the former "wiggle" in the left mid beam antenna response has disappeared, suggesting improved L1b calibration. In the outer swath consistent large departures remain for the uncorrected case. The level 2 monitoring statistics, like average MLE, average wind speed bias with respect to the NWP wind speed, SD of the wind speed and wind direction show almost identical pictures for the PPF630 and PPF620 corrected data.

When using the correction table, the level 2 wind product is of high quality. The aim is to get also a high quality product without using a correction table. Of course, this could be easily achieved by incorporating the correction table in the CMOD fit-parameters. The current results from the ocean calibration for the uncorrected case are not acceptable for a level 2 wind product. This issue should be resolved by checking against other ancillary geophysical data like sea ice or rain forest. This will help in resolving any remaining errors in, and assessing the validity of the currently used CMOD version and L1b calibration, especially for the high incidence angles.

Appendix A1 – Normalisation correction table

- PPF630 to PPF620

The PF630-PPF620 calibration correction factors (dB) as a function of WVC and beam:

```
#  WVC diff_sigma0(dB) fore              mid              aft
    1.          0.0152512910  -0.0013637758  -0.0009096405
    2.          0.0058419360   0.0106227072   0.0712199211
    3.          0.0139260730   0.0254252814   0.0992101580
    4.          0.0375266038   0.0325509869   0.0740866587
    5.          0.0627364814   0.0345954597   0.0236640889
    6.          0.0695543066   0.0434438437  -0.0112409024
    7.          0.0493281409   0.0509052798  -0.0144351749
    8.          0.0200140309   0.0270070396  -0.0070632650
    9.          0.0112696160  -0.0264431052  -0.0150306029
   10.          0.0259555001  -0.0407692492  -0.0281375591
   11.          0.0292403065   0.0356759988  -0.0087748040
   12.          0.0003986195   0.1187243834   0.0474442169
   13.         -0.0190175697   0.0612055175   0.0860490724
   14.          0.0214302465  -0.1131965443   0.0579772480
   15.          0.0878821537  -0.1532246768  -0.0094105024
   16.          0.1033355966   0.0643986166  -0.0339373983
   17.          0.0651476607   0.2651863396   0.0149126789
   18.          0.0073436056   0.1881923974   0.0474765748
   19.         -0.0440768264  -0.0451493524  -0.0140523985
   20.         -0.0216969997  -0.1273071468  -0.0570199154
   21.          0.0720021948  -0.0201749392   0.0096929036
   22.          0.0594572611  -0.0609582998   0.0348240249
   23.          0.0400231145  -0.0284624845  -0.0003434728
   24.         -0.0163168386   0.0822767392  -0.0236283857
   25.          0.0286301672   0.0676115528   0.0261491202
   26.          0.0371050909  -0.0430343412   0.0319797508
   27.          0.0300975032  -0.0599069074  -0.0081544397
   28.          0.0395211354   0.0161063261   0.0080039958
   29.         -0.0062904386   0.0487218164   0.0530108698
   30.         -0.0571108237   0.0111012803   0.0402017646
   31.         -0.0162537694  -0.0177430678  -0.0199473742
   32.          0.0606894717  -0.0072700744  -0.0541118309
   33.          0.0649240687   0.0013216001  -0.0330488645
   34.          0.0080679180  -0.0125664100   0.0113271819
   35.         -0.0204993226  -0.0186375976   0.0408676416
   36.          0.0097813932   0.0005649549   0.0466359779
   37.          0.0491828099   0.0166489501   0.0374469385
   38.          0.0493462719   0.0042296001   0.0235173292
   39.          0.0165073927  -0.0153489290   0.0103901718
   40.         -0.0093309376  -0.0045402655   0.0019900380
   41.         -0.0033473962   0.0306379143   0.0025527684
   42.          0.0245321691   0.0428362116   0.0133182229
```

Appendix A2 – Total correction tables – PPF630

The total calibration correction factors (dB) as a function of WVC and beam:

```
# total correction factors in dB for PPF630
# WVC          fore              mid              aft
   1        0.994154871     0.061118700     0.722670615
   2        0.837909520    -0.035447154     0.621880651
   3        0.690169156    -0.132331967     0.483624995
   4        0.570067644    -0.208910674     0.329411149
   5        0.453513920    -0.272798568     0.177672654
   6        0.310207069    -0.326515496     0.055586006
   7        0.157507062    -0.353697181     0.005338219
   8        0.062825754    -0.334624946    -0.089645557
   9        0.087063208    -0.336839497    -0.221670583
  10       -0.011990754    -0.419735968    -0.201578736
  11        0.008408483    -0.467332661    -0.293766171
  12       -0.128215179    -0.301783115    -0.405724913
  13       -0.119913004    -0.384474993    -0.441223919
  14       -0.233323634    -0.331127614    -0.455675900
  15       -0.232574135    -0.460407078    -0.369246274
  16       -0.288933039    -0.445690006    -0.343044639
  17       -0.310477525    -0.371599585    -0.372309059
  18       -0.169566706    -0.423544616    -0.409216285
  19       -0.136588991    -0.448280275    -0.457410187
  20       -0.219806105    -0.554046869    -0.413682789
  21       -0.192938119    -0.602546155    -0.400480360
  22       -0.233668283    -0.704762638    -0.152654827
  23       -0.203266159    -0.512465179    -0.256590128
  24       -0.247614950    -0.232339770    -0.333496720
  25       -0.196758449    -0.142936468    -0.308634847
  26       -0.238209724    -0.253262073    -0.194429964
  27       -0.152073145    -0.219311535    -0.371747494
  28       -0.199550182    -0.109318301    -0.283815086
  29       -0.263122261    -0.103931531    -0.116151735
  30       -0.219558001    -0.143893510    -0.122604772
  31       -0.173298895    -0.131044760    -0.169698864
  32       -0.089943655    -0.098944224    -0.157650828
  33       -0.079744004    -0.165385470    -0.014688578
  34        0.059277426    -0.232702643    -0.049270120
  35        0.034628745    -0.241925806     0.098884985
  36        0.150072545    -0.221589863     0.183171928
  37        0.262848496    -0.137409776     0.244417191
  38        0.345333904    -0.056014735     0.316448897
  39        0.428960651    -0.013352382     0.415895671
  40        0.559809387    -0.041328192     0.547994912
  41        0.700250626     0.034199350     0.662182808
  42        0.896224856     0.190019637     0.757697761
```

– PPF550

The total calibration correction factors (dB) as a function of WVC and beam:

```
# total correction factors in dB for PPF550
# WVC            fore              mid              aft
    1        0.978903592      0.062482476      0.723580241
    2        0.832067609     -0.046069860      0.550660729
    3        0.676243067     -0.157757252      0.384414822
    4        0.532541037     -0.241461664      0.255324483
    5        0.390777439     -0.307394028      0.154008567
    6        0.240652770     -0.369959325      0.066826910
    7        0.108178914     -0.404602468      0.019773394
    8        0.042811722     -0.361631989     -0.082582295
    9        0.075793594     -0.310396403     -0.206639975
   10       -0.037946254     -0.378966719     -0.173441172
   11       -0.020831823     -0.503008664     -0.284991354
   12       -0.128613800     -0.420507491     -0.453169137
   13       -0.100895435     -0.445680499     -0.527272999
   14       -0.254753888     -0.217931077     -0.513653159
   15       -0.320456296     -0.307182401     -0.359835774
   16       -0.392268628     -0.510088623     -0.309107244
   17       -0.375625193     -0.636785924     -0.387221724
   18       -0.176910311     -0.611737013     -0.456692874
   19       -0.092512161     -0.403130919     -0.443357795
   20       -0.198109105     -0.426739693     -0.356662869
   21       -0.264940321     -0.582371235     -0.410173267
   22       -0.293125540     -0.643804312     -0.187478855
   23       -0.243289277     -0.484002680     -0.256246656
   24       -0.231298119     -0.314616501     -0.309868336
   25       -0.225388616     -0.210548013     -0.334783971
   26       -0.275314808     -0.210227743     -0.226409718
   27       -0.182170644     -0.159404635     -0.363593042
   28       -0.239071310     -0.125424623     -0.291819096
   29       -0.256831825     -0.152653351     -0.169162601
   30       -0.162447184     -0.154994786     -0.162806541
   31       -0.157045126     -0.113301694     -0.149751484
   32       -0.150633126     -0.091674149     -0.103538990
   33       -0.144668072     -0.166707069      0.018360287
   34        0.051209509     -0.220136225     -0.060597301
   35        0.055128068     -0.223288208      0.058017343
   36        0.140291154     -0.222154811      0.136535943
   37        0.213665694     -0.154058725      0.206970245
   38        0.295987636     -0.060244337      0.292931557
   39        0.412453264      0.001996547      0.405505508
   40        0.569140315     -0.036787927      0.546004891
   41        0.703598022      0.003561437      0.659630060
   42        0.871692717      0.147183418      0.744379520
```

– PPF530

The total calibration correction factors (dB) as a function of WVC and beam:

```
# total correction factors in dB for PPF530
# WVC     fore            mid             aft
   1      1.2503467       0.6173953       1.0965289
   2      1.1414015       0.50012696      1.0137894
   3      1.0207639       0.3556557       0.8638302
   4      0.9016627       0.21420181      0.6983539
   5      0.77273965      0.096218154     0.5411821
   6      0.6193935       0.01011885      0.40175956
   7      0.47027808      -0.016497448    0.32280484
   8      0.38249376      0.05376345      0.21661538
   9      0.40001002      0.13122502      0.11744121
  10      0.28815567      0.06967351      0.19709414
  11      0.32885745      -0.07085171     0.14076778
  12      0.2598761       -0.013950959    0.017487556
  13      0.3302297       -0.050653443    -0.037931174
  14      0.203377        0.19449659      -0.036576986
  15      0.12238866      0.1474748       0.0747326
  16      -0.014906973    -0.014204141    0.06432791
  17      -0.08859584     -0.12684219     -0.06618055
  18      0.03551657      -0.1105292      -0.15467502
  19      0.10570371      0.11173591      -0.11362332
  20      0.03940183      0.18098183      0.036361814
  21      0.001832597     0.18216565      0.037807677
  22      0.04173377      0.016276151     0.05322209
  23      0.035736308     -0.07914144     -0.09979808
  24      0.007548481     -0.046546176    -0.19582084
  25      0.012426965     0.05856242      -0.20054713
  26      -0.010088161    0.12159757      -0.021505147
  27      0.118720666     0.22147879      -0.07037181
  28      0.09359506      0.26831436      0.07902609
  29      0.09847376      0.23593642      0.25056392
  30      0.20715716      0.23761165      0.27874148
  31      0.22181079      0.30325115      0.29402766
  32      0.23157474      0.35470447      0.32907492
  33      0.23861948      0.2865908       0.4366482
  34      0.43517822      0.198793        0.350946
  35      0.43907678      0.12745288      0.46996248
  36      0.5198762       0.05631538      0.55271053
  37      0.58201873      0.08414746      0.6248808
  38      0.6452974       0.196938        0.7084997
  39      0.7390548       0.3374183       0.812105
  40      0.8724477       0.40120405      0.9385224
  41      0.98946106      0.5026599       1.0303202
  42      1.1436298       0.6215483       1.0776356
```

— ZZZ

The total calibration correction factors as a function of WVC and beam:

```
# total correction factors in dB for zzz:
# WVC             fore               mid               aft
     1        1.2133132219        0.3155378401        1.0593156815
     2        1.0546579361        0.3271515965        0.8460109234
     3        0.8865517378        0.2479770184        0.6496003866
     4        0.7325554490        0.1451247334        0.4994649887
     5        0.5829378366        0.0331524014        0.3844491839
     6        0.4281365871       -0.0844106078        0.2893532515
     7        0.2965862155       -0.1718853712        0.2391428649
     8        0.2370240837       -0.1716657281        0.1345937848
     9        0.2809681892       -0.1478331089        0.0071905553
    10        0.1794755459       -0.2212673426        0.0310422480
    11        0.2082206905       -0.3234215379       -0.0984380990
    12        0.1067811698       -0.1920946836       -0.2941693366
    13        0.1300185770       -0.1470538378       -0.4001859128
    14       -0.0427028686        0.1610514224       -0.4112668037
    15       -0.1390331388        0.1416956484       -0.2581062615
    16       -0.2424157113       -0.0347604156       -0.1608873904
    17       -0.2293247133       -0.1927063465       -0.1287731230
    18        0.0152223706       -0.2303622365       -0.0443519354
    19        0.1911185235       -0.0541779399        0.1083823442
    20        0.1732259691       -0.0168949366        0.2328085899
    21        0.0853555202       -0.0138236284        0.0146887004
    22       -0.2717875838       -0.2966208458       -0.2114235163
    23        0.2422858775       -0.3946557045        0.2545682192
    24        0.1789116561       -0.1629260182        0.2835853696
    25       -0.0094707310        0.1400903463        0.1562602520
    26       -0.2271785140        0.3288721740        0.1239635944
    27       -0.2178243548        0.4741849899       -0.1162401438
    28       -0.2723082006        0.5029416084       -0.0885529518
    29       -0.2272865176        0.3999486566        0.0379718542
    30       -0.0442254469        0.2948326766        0.0723552704
    31        0.0450129583        0.2533800602        0.1198816299
    32        0.1129163355        0.2297098935        0.1954535246
    33        0.1518224329        0.1440050602        0.3369451165
    34        0.3536116779        0.0978622437        0.2686299086
    35        0.3428944647        0.1023089886        0.3887893260
    36        0.4010559022        0.1011475921        0.4624586403
    37        0.4433895350        0.1553801894        0.5215559006
    38        0.4983410835        0.2290201783        0.5920002460
    39        0.5963876843        0.2703251541        0.6862732172
    40        0.7465131879        0.2189815044        0.8072959781
    41        0.8885478973        0.2612728775        0.8998641968
    42        1.0776052475        0.4263577461        0.9607759118
```

Acronyms and abbreviations

.

Name	Description
AMI	Active Microwave Instrument
ASCAT	Advanced scatterometer
AWDP	Ascat Wind Data Processor
BUFR	Binary Universal Form for Representation (of meteorological data)
CMOD	C-band geophysical model function used for ERS and ASCAT
ECMWF	European Centre for Medium-Range Weather Forecasts
ERA40	ECMWF 40 year reanalysis
ERS	European Remote sensing Satellite
ESA	European Space Agency
ESDP	ERS Scatterometer Data Processor
EUMETSAT	European Organization for the Exploitation of Meteorological Satellites
GMF	geophysical model function
KNMI	Koninklijk Nederlands Meteorologisch Instituut (Royal Netherlands Meteorological Institute)
METOP	Meteorological Operational satellite
MLE	maximum likelihood estimator (used for distance to cone)
NWP	numerical weather prediction
OSI	Ocean and Sea Ice
QC	Quality Control (inversion and ambiguity removal)
SAF	Satellite Application Facility
SD	standard deviation
WVC	wind vector cell, also known as node or cell

Table 1 - List of acronyms and abbreviations

References

[FIGA 2004] Figa-Saldaña, Julia, "ASCAT calibration and validation plan", *EUMETSAT*, EPS programme, Darmstardt Germany, 2004

[FIGA et al 2002] Figa-Saldaña, J., J.J.W. Wilson, E. Attema, R. Gelsthorpe, M.R. Drinkwater, and A. Stoffelen, The Advanced scatterometer (ASCAT) on the meteorological operational (MetOp) platform: A follow on for the European wind scatterometers, Can. J. Remote Sensing *28 (3)*, pp. 404-412, 2002.

[HERSBACH 2003] Hersbach, Hans, "CMOD5 An improved geophysical model function for ERS C-band scatterometry, *Technical Memorandum 395, ECMWF*, Reading GB, 2003

[HERSBACH et al 2007] Hans Hersbach, Ad Stoffelen, Siebren de Haan, CMOD5, J. Geophys. Res. , accepted.

[PORTABELLA and STOFFELEN 2006] Marcos Portabella, Ad Stoffelen, Scatterometer backscatter uncertainty due to wind variability, IEEE Trans. Geosci. Rem. Sens. **44** (11), 3356-3362, 2006.

[PORTABELLA and STOFFELEN 2007] Portabella, M., and Stoffelen, A., "On scatterometer ocean stress," submitted to *J. Atm. and Ocean Techn*. in June 2007, © American Meteorological Society

[STOFFELEN 1999] Stoffelen, Ad, "A Simple Method for Calibration of a Scatterometer over the Ocean", J. Atm. and Ocean Techn. 16(2), 275-282, 1999.

[STOFFELEN 1998] Stoffelen, Ad, "Scatterometry", KNMI*, PhD thesis at the University of Utrecht*, ISBN 90-39301708-9, October 1998

[STOFFELEN and ANDERSON 1997] Stoffelen, Ad, and David Anderson, "Scatterometer Data Interpretation: Measurement Space and inversion", J. Atm. and Ocean Techn., 14(6), 1298-1313, 1997.

[VERHOEF et al 2008] Verhoef, A., M. Portabella, A. Stoffelen and H. Hersbach, "CMOD5.n - the CMOD5 GMF for neutral winds", OSI SAF Technical Report SAF/OSI/CDOP/KNMI/TEC/TN/165, 2008

[VERSPEEK 2006] Verspeek, Jeroen, "Scatterometer calibration tool development", EUMETSAT Technical Report SAF/OSI/KNMI/TEC/RP/092, *KNMI*, de Bilt, 2006,

[VERSPEEK 2006-2] Verspeek, Jeroen, "User manual Measurement space visualisation package", *KNMI*, de Bilt, 2006